Exploitation of Harmonic Generation in Time-Controlled Frequency Diverse Arrays for WPT

# Exploitation of Harmonic Generation in Time-Controlled Frequency Diverse Arrays for WPT

Tommaso Tiberi, *Student Member, IEEE*, Enrico Fazzini, *Student Member, IEEE*, Alessandra Costanzo, *Fellow, IEEE,* and Diego Masotti, *Senior Member, IEEE*

***Abstract*—This work presents a novel and detailed harmonic analysis of Frequency Diverse Arrays (FDAs) when a pulsed regime is adopted to resolve the typical range-angle coupling of their radiation mechanism. This analysis demonstrates the positive exploitation of the harmonic generation of time-controlled FDAs when their use as smart energy sources for Wireless Power Transfer applications is envisaged: in this contest, several pulse waveforms are compared and the delicate trade-off between the minimization of the power dispersed among out-of-band harmonics and the confinement of the illuminated region of space is deeply discussed. The triangular-shaped pulse combined with its repetition frequency identical to the constant frequency spacing among the antennas results to be the most promising choice. The analytical results are supported by measurements carried out in a realistic scenario with a 4-monopole planar array operating at 1.8 GHz.**

***Index Terms*—Active antenna array, harmonic analysis, beamforming, wireless power transfer.**

## I. Introduction

THE NEED for precise radiation of the signal/power in the region where the target is positioned represents one of the main bottlenecks for the feasibility of far-field wireless transmission of the power (WPT) [1]. This has pushed the interest of researchers on advanced radiating architectures to overcome this problem [2, 3].

In the last years, special attention has been devoted to Frequency Diverse Arrays (FDAs), i.e., coherent radiation of signals with slightly different frequencies [4]: this new degree of freedom (the frequency spacing of the array elements excitations) leads the array factor of FDAs to be dependent on the distance, angle and time.

The simultaneous range and angle dependency is the added value of FDAs, since it allows to perform beam steering without the need of phase shifters, adopted in traditional phased arrays. Afterwards, FDAs have been proposed for WPT applications, both for long-range [5] and indoor scenarios [6]. To this aim, improvements on the geometry of the radiating architecture both for linear [7] and bi-dimensional arrays [8], [9], and on the frequency offset distribution [10], [11] have been proposed to enhance the spot accuracy. The time dependency of the radiation mechanism makes the FDAs suitable for radar applications, which has been their original exploitation, because of their intrinsic scanning capability [12], but introduces some challenges if WPT scenarios are concerned.

This time-dynamic pattern has been subject to many studies, from different perspectives within the research community with the purpose to fix the radiated spot in time. For example, a delicate optimization of the frequency offset distribution has been adopted in [13] to counteract the dynamicity of the FDA pattern, at the expense of an unfeasible increasing complexity of the signal generation system. An alternative and simpler approach [14], [15] pursues the duty-cycling of the radiation of each diverse-in-frequency element through a rectangular pulse: this radiation control transfers the complexity to the piloting part of the system, where a Software Defined Radio can easily do the job, as claimed for the first time in [6], where an indoor WPT scenario was considered. However, as firstly highlighted in [16], [17,] a common misconception of the pulsed FDA radiative behavior is observed if the pulse propagation is not accounted for. Indeed, an apparent control over time of the FDA pattern seems possible, but the resulting prediction is not consistent since the carrier and the pulse waveforms result to obey to different and uncorrelated time propagation laws. Vice versa, when pulse modulation is applied to the transmitting FDA, each harmonic of the pulsed signal is processed in the same way by the channel. According to this correct perspective, a pulsed FDA allows to restrict the typical S-shape pattern in a confined angular sector, and, by varying the pulse delay, beam steering on demand can be performed. Therefore, the obtained radiating system operates similarly to an advanced phased array, with reduced architecture complexity, since the role of the phase shifter is substituted by a simple switch, hence it is still worthy of attention.

In particular, the control of the antennas excitation through a pulse waveform is responsible for the generation of harmonic products due to the intermodulation of the carrier(s) signal(s)

Manuscript submitted on 5 April 2023.
This work was partly funded by the Italian Ministry of Education, University and Research (MIUR) within the framework of the PRIN 2017-WPT4WID ("Wireless Power Transfer for Wearable and Implantable Devices") and partly by the European Union through the Italian National Recovery and Resilience Plan (NRRP) of Next Generation EU, partnership on "Telecommunications of the Future" (Program "RESTART") under Grant PE00000001.
Tommaso Tiberi, Enrico Fazzini and Diego Masotti are with DEI, Alma Mater Studiorum Università di Bologna, Bologna, 40136, Italy. (e-mail: tommaso.tiberi@unibo.it, enrico.fazzini2@unibo.it, diego.masotti@unibo.it).
Alessandra Costanzo is with DEI, Alma Mater Studiorum Università di Bologna, Cesena, 47522, Italy (e-mail: alessandra.costanzo@unibo.it).

with the control frequency of the on-off sequences. This is a well-known phenomenon deeply studied in another family of smart radiating architectures, the time-modulated arrays [18], [19], whose radiating peculiarity exactly relies on the multi-frequency generation, that has been successfully exploited also for WPT purposes [20], [21]. The loss of power because of the presence of uncontrolled sideband harmonics has also been studied for this family of arrays [22], [23].

Despite this, the time-controlled FDA (TCFDA) has been studied in the sole time-domain, up to now. This paper tries to bridge this gap, by providing, for the first time, an exhaustive analysis in the frequency domain of the complex radiation mechanism of these arrays, leading to the accurate evaluation of the amount of power lost because of this phenomenon. This analysis demonstrates that the harmonic generation due to the synchronous on-off of the antennas excitations results in an insurmountable obstacle for communications purposes. On the other hand, when these arrays are adopted for WPT purposes, this work demonstrates that the harmonics generation can be favorably exploited. Moreover, the proposed analytical approach allows to perform a careful choice of the driving pulse waveforms thus leading, for the first time, to the comparison of different driving sequences and their effects on both the loss of power, due to the harmonic generation, and the shape quality of the covering spot of space for TCFDA architectures.

The results of the theoretical analysis are validated by a measurement campaign, carried out in laboratory premises, in order to validate the smart radiating strategy in indoor scenarios: for this purpose, a planar array of 4 monopoles resonating at 1.8 GHz is adopted. Of course, the optimum focusing distance is forced to be close to the transmitting array, for the limited availability of space: but this does not affect the general-purpose nature of the proposed array design results.

The paper is organized as follows: in section II an overview on the main features of TCFDA is provided, followed by the problem statement regarding the pulse harmonics generation and its impact on the system radiating behavior. Then, an exhaustive power spectral analysis on the TCFDA signals is carried out in section III, and the Power Loss figure of merit is defined. This parameter, being a key performance indicator for TCFDA systems, is derived and properly characterized with respect to several working scenarios examined in this work. Afterwards, in section IV, three main types of pulses to realize the direction-control of the FDA radiation pattern are investigated and compared. In section V a description of the carried-out measurement activity and the validation of the developed theory is reported, and the final conclusions are drawn.

## II. Time Controlled Frequency Diverse Arrays

In this section a novel investigation on the radiating properties of time-controlled frequency diverse arrays (TCFDA) is proposed. The peculiarity of these radiating systems stands in the pulse modulation technique applied to the continuous waveform (CW) excitation signals to be radiated by the array. The macroscopic effect of this excitation format enables a unique angular control of the FDA radiation pattern.

As pointed out in previous works [12], the S-shape beam pattern is a typical property of standard FDAs (i.e. linear array with linear frequency diversity), resulting in a strong range-angle coupling of the radiation pattern: at a given time instant, by varying the scanning angle, the signal is focused at different distances from the source. This dynamic behavior is a useful feature for radar and localization purposes. However, for WPT applications a robust control of the system's radiation is mandatory, to intentionally transfer power in desired directions only, according to the position of targets to be energized. For this reason, a time-control strategy, based on pulse modulation has been coupled with the standard FDAs excitation, to pursue a collapse of the "S-shape" in favour of angle-confined radiation and definitely resolve the tough mutual dependency between range and direction. Fig. 1 shows standard FDA beam patterns for WPT scenarios, hence with the "S" spanning regions of tens of meters (instead of km, as for radar applications, as better explained later): Fig. 1(a) represents the evolution over time of the FDA pattern in a theta-time graph (for $r = 0\,m$), the superimposed pulsed signal is also shown. Whereas Fig. 1(b) depicts the radiation pattern in a range-theta graph at fixed time instant $t = 0\,ns$ (i.e. in the instant of transmission).

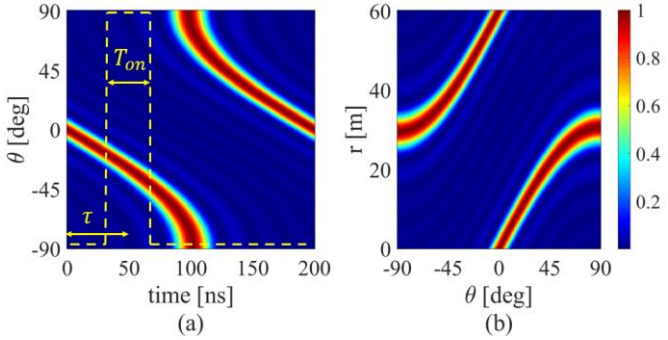


Fig. 1. Normalized standard FDA beam pattern: (a) time-varying behavior and superimposed pulse (dashed line) with on-time $T_{on} = 20\,ns$ and delay $\tau = 50\,ns$. (b) range-angle pattern at fixed time instant $t = 0\,ns$.

In this way, the overall signal transmitted by the array is not a CW anymore, but may be cast as:

$$x(t) = x_{pulse}(t-\tau)\sum_{m=0}^{M-1} e^{j2\pi f_m t} \tag{1}$$

where $x_{pulse}$ represents the pulse waveform, $f_m$ is the operating frequency of the $m^{th}$ antenna and $M$ is the number of array elements. The pulse shape design requires specific settings, such as the periodicity $T$, the on-time $T_{on}$ and the delay $\tau$. These parameters are fundamental degrees of freedom to select the desired time-slots of radiation, in order to achieve the two-fold goal of maximizing power transmission in precise directions from the source and cancelling radiation in unwanted space regions. For example, by setting a pulse delay $\tau = 50\ ns$ as in Fig. 1(a), the main beam is steered around -30 degrees, with respect to the broadside direction. Without loss of generality, the analysis carried out in this work refers to a scenario in which the target is in the broadside direction with respect to the energy source, therefore a delay $\tau = 0\ ns$ is considered. Anyway, it can be proved that the same analysis can be extended to whatever direction of transmission, by adjusting the value of τ accordingly. Indeed, this time-control technique allows to achieve ad-hoc and real time WPT and represents a consistent solution to nimbly handle the FDAs beam pattern. To better visualize the radiating behavior of the TCFDA system, multiple snapshots of the beam pattern have been collected at different time instants and reported in Fig. 2.

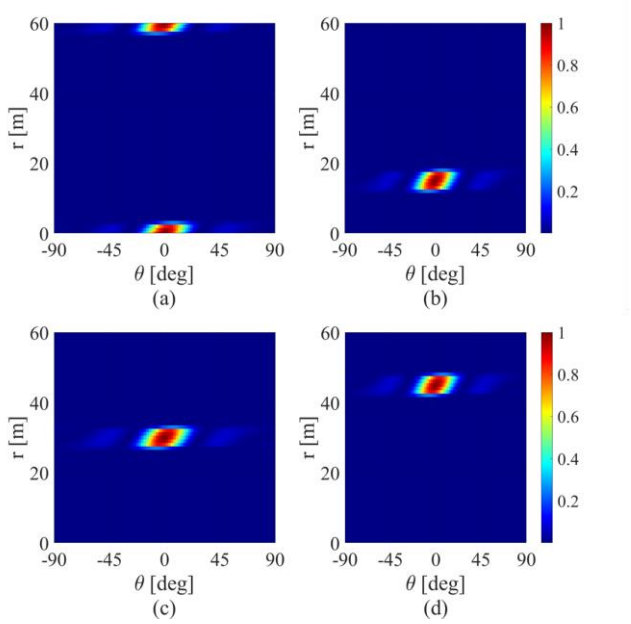


Fig. 2. Normalized TCFDA beam pattern (with rectangular pulse effect) at: (a) $t = 0\ ns$, (b) $t = 50\ ns$, (c) $t = 100\ ns$, (d) $t = 150\ ns$.

The movement over time of the radiation is well visible, even though the pulse modulation allows to restrict the transmission in a limited direction only, representing a great advantage with respect to the standard scenario (Fig 1(b)) when intentional and precise power transfer is pursued. However, up to now the performance of TCFDA has been investigated with respect to the time domain, only, while a novel interesting perspective is offered by the frequency spectra of the pulsed FDA that is discussed in the following.

Let us consider a linear array of $M$ antennas, aligned along the $x$ axis, as reported in Fig. 3. It is worth mentioning that the deployment of more sophisticated array layouts, such as a

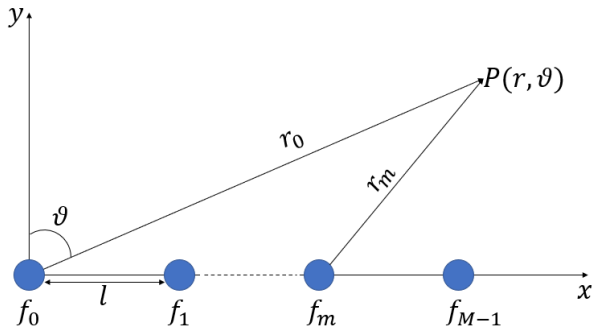


Fig. 3. M-element linear array aligned along $x$ axis.

logarithmic inter-element distribution [7] or a planar arrangement of the elements, both in a rectangular [24] and in a circular [8],[9] shape, leads to a beam spot naturally confined in a more limited region, thus strongly reducing the usefulness of the pulse-based technique. For this reason, the paper focuses on a standard linear array layout.

Frequency diversity is introduced among the elements according to the following rule:

$$f_m = f_0 + m\Delta f\ , (m = 0, \dots, M-1) \qquad (2)$$

where $f_0$ is the operating frequency of the zero element ($m = 0$) and $\Delta f$ is the constant frequency offset among consecutive elements. $l$ indicates the spacing among adjacent antennas and $r_m$ describes the distance between the $m^{th}$ antenna and the target point $P$. Supposing to work in far-field conditions, the following approximation holds:

$$r_m = r_0 - (m \cdot l)\ sin(\vartheta) \qquad (3)$$

In a standard FDA system, where CW signals are involved, the spectrum is occupied by the fundamental tones only, as represented in Fig. 4.

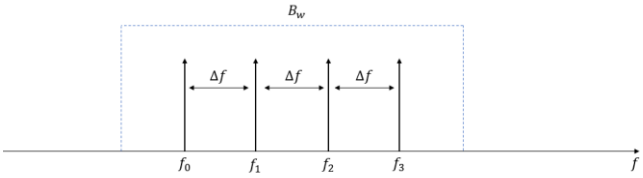


Fig. 4. Spectrum of a standard FDA (M=4).

With the introduction of the pulse signal modulating the predefined continuous waveforms, the spectrum inherently contains infinite harmonic components associated to each fundamental signal, as visible in Fig. 5, where $f_p = 1/T$ is the pulse frequency, that defines the spacing between adjacent harmonic tones. Therefore, the frequency characterization of pulsed FDA is more complex, but absolutely needed.

In particular, the harmonic analysis can be performed either focusing on information transmission or on power transmission. For what concern communication purposes, the harmonic terms generated by the pulse modulation are definitely dangerous for the quality and reliability of the network. Indeed, a fundamental condition must be respected:

$$(M-1)\Delta f < f_p \tag{4}$$

The left-hand side term of (4) defines the frequency distance between the lowest and the highest fundamental tones of a M-elements FDA. If condition (4) is satisfied, the first side-bands (i.e. harmonic order equal to 1) of $f_m$ satisfy the following inequalities:

$$f_m + f_p > f_{M-1} \qquad (m = 0, \dots, M-1) \tag{5}$$

$$f_m - f_p < f_0 \qquad (m = 0, \dots, M-1) \tag{6}$$

In this way, co-channel interference is avoided because the harmonic terms are distributed in such a way that they fall outside the channel bandwidth $B_w$ ,which is an essential condition to be satisfied for a safe data communication. Moreover, a pass-band filter must be introduced to minimize adjacent channel interference with other users. Unfortunately, due to the high number of harmonics, significant amount of radiated power is distributed at those frequencies. Therefore, huge power losses are encountered on the side-band harmonics. This working condition introduces a critical obstacle for the feasibility of TCFDA, that could not be a reliable technique anymore if exploited for communication purposes.

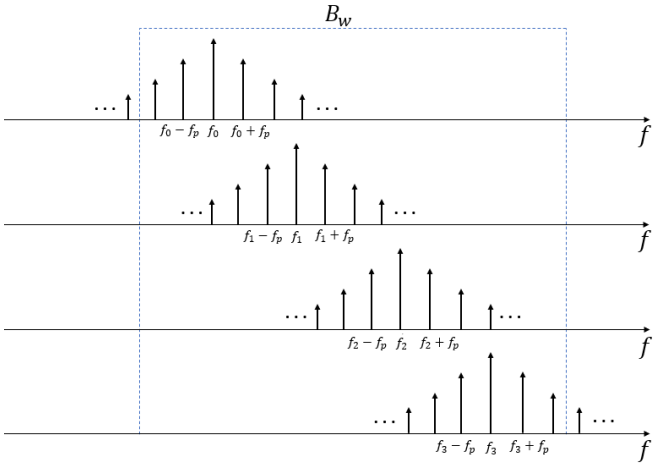


Fig. 5. Spectrum of a pulsed FDA (M=4).

However, the aim of this work is to propose a different perspective suitable for WPT applications. Indeed, if TCFDA are adopted for power transmission the condition (4) can be violated, to promote the deployment of harmonic terms within $B_w$ (i.e. improving the power distribution over the band of interest). In this way, the intrinsic pulse harmonics are positively exploited for powering purposes, thus minimizing the power loss, as detailed in the following analysis.

A further motivation to violate (4) in WPT applications comes from a hardware constraint regarding the multi-frequency generation. Let us consider the system depicted in Fig. 6. The CW signal at the output of the generator is processed by a pulse wave modulator (PWM), and the obtained pulsed signal is then radiated by the antenna. The design parameters $(\tau, T_{on})$ of the pulse play an essential role to handle the behavior of the FDA radiation (described in Fig. 1).

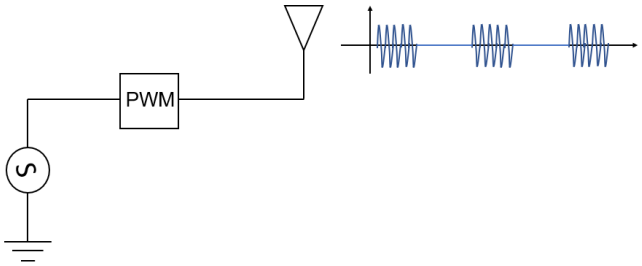


Fig. 6. Scheme of one channel responsible for the signal generation in a TCFDA architecture.

A first consideration regards the relationship between the time periodicities of the pulse and the FDA pattern. The second one fixes the maximum time window of interest to $1/\Delta f$. If $f_p$ exceeds $\Delta f$, the pulse signal repeats more than once within an FDA period, and the unique correspondence $(\tau, T_{on})$-angle of Fig. 1(a) is lost. This means that the system is going to radiate in different directions within a single period, whereas the focus of this work is to characterize the harmonic contributions of a single pulsed FDA beam (i.e. the direction of transmission is one and fixed). Therefore, the frequency offset $\Delta f$ represents an upper bound for the pulse periodicity and the following additional condition must be set:

$$f_p \leq \Delta f \tag{7}$$

On the other hand, a lower bound for $f_p$ cannot be specified. However, the designer must be aware that increasing the time periodicity of the pulse, keeping $T_{on}$ and $\tau$ parameters (therefore, the steering direction and dimension of the focusing area) fixed would imply a reduced amount of power delivered to the target (e.g., a rectenna), because of the longer silent period. This aspect will be detailed in the following through the definition of a proper figure of merit related to the transfer of power.

## III. Power Analysis of Time-Controlled FDA Signals

The generic pulse signal, that modulates the CW signals generated by the antennas, can be expressed according to its Fourier series expansion:

$$x_{pulse}(t) = \sum_{n=-N_H}^{N_H} C_n e^{j2\pi n f_p t} \tag{8}$$

Where $N_H$ is the number of harmonic terms characterizing the pulse, and $C_n$ are the Fourier coefficients of the pulse, that can be expressed as:

$$C_n = \frac{1}{T}\int x_{pulse}(t) e^{-j2\pi n f_p t} dt \ , \ (n = -N_H, \dots, N_H) \tag{9}$$

Then, the generic signal transmitted by the $m^{th}$ antenna can be written as:

$$x_m(t) = e^{j2\pi f_m t} x_{pulse}(t) = e^{j2\pi f_m t} \sum_{n=-N_H}^{N_H} C_n e^{j2\pi n f_p t} \quad (10)$$

Being $x_m(t)$ a periodic signal, the average signal power can be computed as:

$$P_{x_m} = \sum_{n=-N_H}^{N_H} \left| C_n e^{j2\pi (f_m + n f_p) t} \right|^2 \quad (11)$$

Finally, the total signal radiated by the array is:

$$x(t) = \sum_{m=0}^{M-1} e^{j2\pi f_m \left(t - \frac{r_m}{c}\right)} \sum_{n=-N_H}^{N_H} C_n e^{j2\pi n f_p \left(t - \frac{r_m}{c} - \tau\right)} \quad (12)$$

Since $x(t)$ is a periodic signal as well, the total average signal power is given by:

$$P_x = \sum_{m=0}^{M-1} \sum_{n=-N_H}^{N_H} \left| C_n e^{j2\pi (f_m + n f_p) \left(t - \frac{r_m}{c} - \tau\right)} \right|^2 \quad (13)$$

Once the total power $P_x$ is characterized, an effective figure of merit named Power Loss can be derived and defined as:

$$P_{loss}[\%] = \left(1 - \frac{P_{x_{Bw}}}{P_x}\right) \cdot 100 \quad (14)$$

where $P_{x_{Bw}}$ denotes the total average signal power within the bandwidth of interest $B_w$. $P_{loss}$ quantifies the amount of power lost on the side-band harmonics with respect to the total available power. This quantity is strictly dependent by the bandwidth $B_w$ of the system.

A simulation example of TCFDA system with $M = 4$, $f_0 = 1.8\ GHz$ and $\Delta f = 5\ MHz$ is proposed. This choice of $\Delta f$ in the order of MHz is typically adopted for WPT purposes, to obtain RF power concentration at tens of meters from the transmitter, as can be evinced from the "S-shape" spanning of Fig. 1(b) [6]. However, the FDA principle is still valid for lower $\Delta f$, e.g. in the order of kHz, to achieve scanning distances of km, envisaged for radar applications.

As a starting point, the $P_{loss}$ as a function of the duty-cycle is reported in Fig. 7, considering a $B_w$ of 100 MHz and $f_p = 20\ MHz$. The choice of a value of $f_p$ greater than $\Delta f$ and in accordance with (4) for a communication scenario, but generating more than one maximum in the FDA period (hence, violating (7)) is also responsible for high power losses due to the out-of-band harmonics. In fact, considering small values of the pulse duty cycle (e.g., $0.1 \div 0.2$), typical of TCFDA systems because they directly impact on the size of the beam spot, the achieved $P_{loss}$ levels are definitely high (around $50 \div 60\ \%$), and the majority of the transmitted power is wasted on side-band harmonics.

To preserve the strength of the pulse-based time control technique, a minimization of the $P_{loss}$ parameter must be pursued. Indeed, design choices for the pulse design play a crucial role for the optimization of the system performance with respect to power transmission.

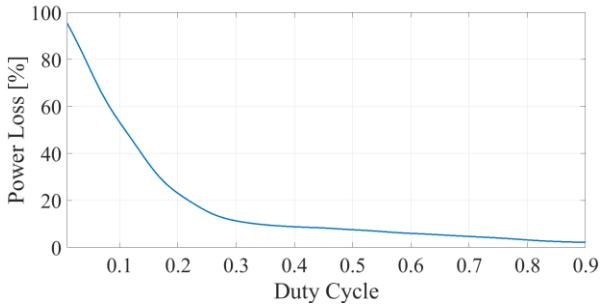


Fig. 7. Power Loss curve with a rectangular pulse, $f_p = 20\ MHz$ and $B_w = 100\ MHz$.

## IV. Power Loss Comparison for different Pulse Shapes

In this section, an investigation on different pulse waveforms modulating the FDA signals is discussed. Then, the performance of the corresponding TCFDA systems are derived. As mentioned before, the pulse properties strongly affect the behavior of the TCFDA radiation.

Let us consider the same scenario presented in section II: a linear array of $M = 4$ antennas, with $f_0 = 1.8\ GHz$ and $\Delta f = 5\ MHz$. The bandwidth of interest is set to $B_w = 100\ MHz$, being in accordance with typical values of operating bandwidth of antenna arrays, realized in planar technology in the microwaves range. An interesting scenario for WPT is found setting $f_p = \Delta f = 5\ MHz$, hence respecting (7). In this case, the lower order harmonics of each fundamental frequency $f_m$ are coincident with the adjacent fundamentals, as visible in Fig. 8.

Since information distortion is not a concern anymore, the harmonic radiation can be positively exploited to promote the power distribution within $B_w$, thus minimizing the $P_{loss}$. The time-control technique with different pulse shapes is applied to the FDA system, and its performance in terms of $P_{loss}$ are discussed.

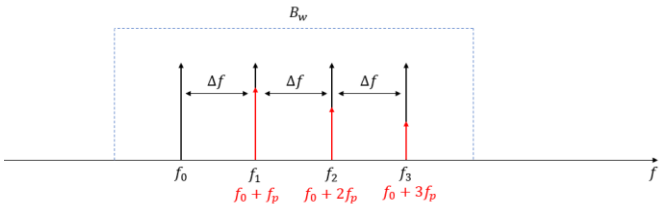


Fig. 8. Spectrum pulsed FDA (M=4), $f_p = \Delta f$. Harmonics (red lines) superimposed to the fundamental tones (black lines).

### A. *Rectangular pulse*

A rectangular pulse characterized by an amplitude $A = 1$ and a duty cycle $d = \frac{T_{on}}{T}$, can be expressed in terms of its Fourier expansion:

$$x_{rect}(t-\tau_{rect}) = \sum_{n=-N_H}^{N_H} C_n^{rect} e^{j2\pi n f_p (t-\tau_{rect})} \quad (15)$$

with $C_n^{rect} = A \cdot d \cdot sinc(nd)$ and $T = \frac{1}{f_p}$.

In Fig. 9, the Power Loss behavior (blue line) is reported.

A straight comparison with the previous case (Fig. 7) highlights that the amount of dissipated power is strongly minimized, proving the effectiveness of TCFDA for WPT applications. Indeed, fixing the duty cycle to 0.1 (i.e. 10 % of $T$) which correspond to an illuminated region of around 24 degrees as reported in Fig. 10(a), the $P_{loss}$ is close to 9 %.

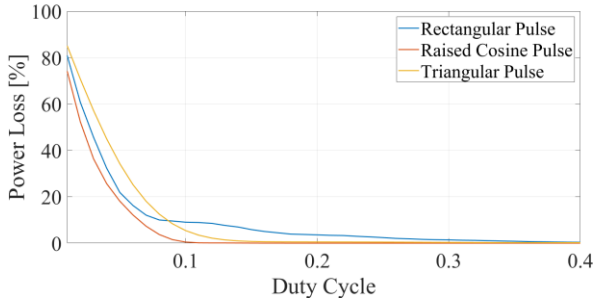


Fig. 9. Power Loss vs Coverage for various TCFDA configurations: (blue) rectangular pulse, (red) raised cosine pulse, (yellow) triangular pulse.

### B. *Raised cosine pulse*

A raised cosine waveform has been considered and tested for the first time in the framework of a TCFDA system. For this control signal the roll-off factor $\alpha$, is a key choice for the pulse design: for $\alpha = 0$, the pulse coincides with a rectangular one, while for decreasing $\alpha$ a smoother transition between the pulse states is obtained. Since it is well-know how the duration of the pulse transitions increases with increasing values of $\alpha$, to set a unique definition of the pulse duty cycle, independent from $\alpha$, the pulse on-time corresponds to the time window where the raised cosine pulse is greater than 0.5. In this way $T_{on}$ is always the same, irrespective of $\alpha$, and the duty-cycle is derived accordingly.

The simulation results of the TCFDA adopting $\alpha = 1$, superimposed in Fig. 9 (red line) with those adopting $\alpha = 0$, demonstrate that the smooth shape of such waveform, results in spectral components quite relaxed which positively contribute to the reduction of $P_{loss}$. In this case, with duty cycle of 0.1 the $P_{loss}$ drops below 1 %.

### C. *Triangular pulse*

The accuracy of the time-control technique can be significantly improved through the novel introduction of a triangular pulse, replacing the rectangular one. A triangular waveform is obtained by the convolution between two identical rectangular pulses:

$$x_{tri}(t-\tau_{tri}) = x_{rect}(t-\tau_{rect}) * x_{rect}(t-\tau_{rect}) \quad (16)$$

where * indicates the time domain convolution among two

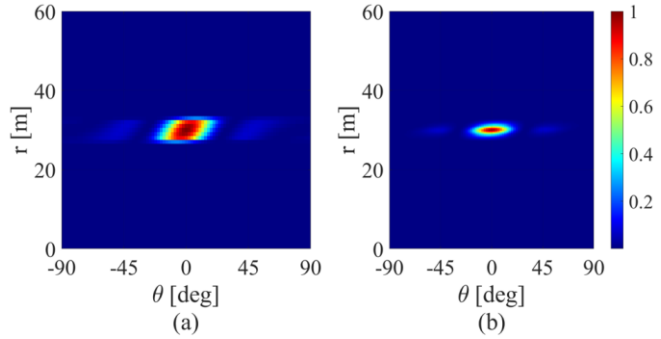


Fig. 10. Normalized TCFDA beam pattern: (a) rectangular pulse (b) triangular pulse, with time fixed at $t = 100\ ns$, $T_{on} = 20\ ns$, and $\tau = 0\ ns$.

signals. $\tau_{rect}$ and $\tau_{tri}$ represent the delay applied to the rectangular and triangular pulses respectively. In accordance with the Fourier properties of the convolution, the resulting triangular waveform has a double delay with respect to the original rectangular wave ($\tau_{tri} = 2 \cdot \tau_{rect}$), while preserving the same periodicity. Even though for this novel waveform the duty cycle definition is not straightforward, the on-time has been computed as the time interval where the triangular pulse is different from zero, coherently with the rectangular case. Therefore, the duty cycle definition remains unchanged. The time-control technique based on a triangular pulse modulation leads to an extremely precise power focusing. A triangular signal reaches the peak in a single time instant, therefore the radiating spot is confined in a precise and restricted region. By selecting properly the value of $\tau_{tri}$, maximum power focusing is guaranteed in the target direction, significantly reducing the energy wasted in surrounding regions. The energy awareness of this solution, compared to the common one based on a square pulse, is shown in Fig. 10(b), where the enhanced selectivity of the power spot for TCFDA involving the triangular pulse is evident. In this use case, both pulses have been chosen of duration 20 ns and delay $\tau = 0\ ns$, to achieve maximum power in broadside direction, as visible in Fig. 10.

The triangular pulse is characterized by a reduced harmonic content, with respect to the rectangular one resulting in a lower $P_{loss}$ thus improving the TCFDA performance, as shown in Fig. 9 (yellow line) with a duty cycle of 0.1, corresponding to $P_{loss} = 5.4$ %.

## V. TCFDA Performance Analysis

### A. *TCFDA performance comparison*

By comparing the simulation results adopting the various pulses (Fig. 9), the TCFDA based on raised cosine pulse with $\alpha = 1$ guarantees the highest $P_{loss}$ reduction. While, from the beam spot perspective, the triangular pulse provides the most accurate radiation mechanism. Furthermore, it can be observed that for a fixed bandwidth of 100 MHz, the main parameter affecting $P_{loss}$ is the pulse duty cycle, whereas the pulse shape modifies $P_{loss}$ by few percents only (e.g. 5.4 % for the triangular pulse compared to approximately 1 % for the raised cosine). Overall, since $P_{loss}$ values below 10 % are fine from the harmonic exploitation viewpoint, the TCFDA system

based on triangular pulse modulation is proposed as the most promising choice, due to its enhanced selectivity of the radiating spot (Fig. 10(b)). As long as the main system's requirement is set by the angular accuracy of the FDA radiation, the choice is oriented towards selective waveforms like the triangular one. Vice versa, if the main goal of the radiating system is to pursue a $P_{loss}$ minimization, smoother waveforms, as a raised cosine pulse, should be adopted. Obviously, the $P_{loss}$ drops very fast for increasing values of the duty cycle since the system tends to a continuous regime (reached when $d = 1$) and the harmonic terms start to vanish. However, in order to guarantee an effective direction-control of the FDA radiation pattern the pulse duty cycle must be kept pretty low [25], usually around 0.1 when frequency spacing in the MHz order are involved. Once this requirement is met, the resulting TCFDA architecture can be suitably exploited for accurate WPT. Further considerations and performance analysis supported by experimental results are presented in the following sections for the various TCFDA solutions.

### B. *Powering Effectiveness*

A different investigation on the TCFDA behavior can be made by varying the periodicity of the pulse $T = 1/f_p$, whereas the amplitude of the transmitted signals and the on-time of the pulse are considered fixed (the latter equal to 20 ns) to preserve the effectiveness of the TCFDA technique despite the time variability of the pattern. To evaluate the power transfer capability of the system, a new figure of merit, the Powering Effectiveness, is introduced:

$$Powering\ Effectiveness = \frac{P_{x_{B_w}}}{P_{B_w}^{max}} \cdot \frac{T_{obs}}{T} \qquad (17)$$

where $T_{obs}$ is the observation time in which the powering process is analyzed ($T_{obs} \gg T$), and $P_{B_w}^{max}$ is the maximum amount of power that can be transmitted, once the on-time and the delay of the pulse are fixed.

The results for different $f_p$ values for a rectangular pulse shape, presented in Fig. 11, highlight how a higher value of the pulse periodicity allows to deliver a higher amount of power, simply because the system is active for a longer period. The value of 5 MHz is considered as the best scenario, since it represents the maximum that $f_p$ can reach in accordance with (7), and therefore leads to a maximization of the Powering Effectiveness. Indeed, a normalization of the Powering Effectiveness with respect to its maximum (corresponding to $f_p = 5\ MHz$) is performed and the resulting curve is shown in Fig. 11.

It is worth noting that the exploitation of pulsed-FDA instead of traditional phased-arrays, when WPT scenarios are foreseen, is advantageous because of the simpler and more agile architecture, as previously stated; but this holds from the powering point of view, too, despite of the pulsed nature of the radiation. In fact, the pulse maximum power content of a TCFDA can be increased with respect to the one radiated by a phased-array, provided that the total mean value in a time-period remains below the regulation limits. In this way, a generic battery-less sensor can profitably exploit the precise and periodically transferred amount of RF power sent to its location. Indeed, let us consider a rectifying antenna (rectenna) [26], supporting the energy needs of the sensor, consisting of a voltage doubler loaded by the parallel connection of a 10 pF capacitance and a 1 kΩ resistance. In this case the time constant for charging the load (which represents either the rectenna optimum load or the equivalent impedance of a power management unit (PMU)) is 10 ns. In this case the 20 ns duration of the pulse allows to guarantee an effective charging transient (almost 90 % of the maximum charged state), according to the experimental results of [26]. Furthermore, the pulsed nature of TCFDA signals (different from the continuous regime of a phased array) with high peak to average power ratio (PAPR) is very useful in ultra-low power applications like wake-up radio (WuR) solutions [27], since the sensitivity of a WPT receiver device could be noticeably boosted.

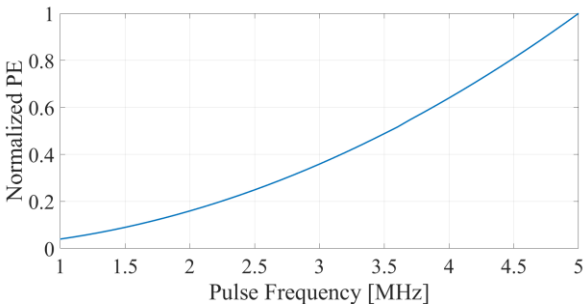


Fig. 11. Normalized Powering Effectiveness vs Pulse Frequency

## VI. Measurement Set-Up and Performance Validation

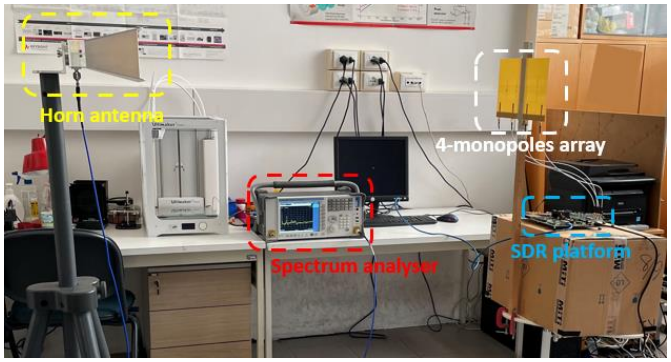


Fig. 12. Measurement set-up in an indoor environment.

A measurement campaign has been conducted to validate the simulation results. An antenna array of 4 monopoles resonating at 1.8 GHz is used as the power transmitter, while at the receiver a horn antenna (TDK RF SOLUTIONS HRM-0118) is used. A Software Defined Radio (SDR) platform (Xilinx Zinq RFSoC) is adopted to generate and control simultaneously the signals transmitted by each antenna, according to the FDA principle. A frequency offset $\Delta f = 5\ MHz$ is used among the array elements: hence the radiated frequencies are 1.8 GHz, 1.805 GHz, 1.810 GHz, 1.815 GHz. Measurements have been carried out considering a link distance of 1.5 m (due to the space constraints of the

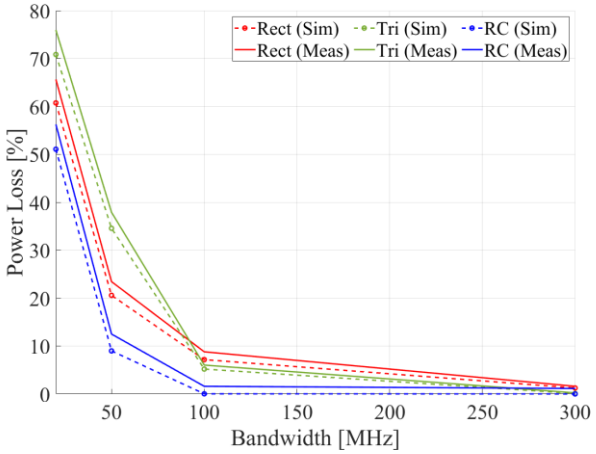


Fig. 13. Power Loss vs bandwidth: simulations and measurements results (rectangular pulse (red), triangular pulse (green), raised cosine pulse (blue)).

laboratory premises, but still guaranteeing the fulfilment of the far-field conditions) where the receiving antenna is located in broadside direction with respect to the transmitting one. Therefore, the pulse signals, to excite the TCFDA, have been designed accordingly. A photo of the system set-up is shown in Fig. 12.

Before presenting measurements results, some considerations about the usage of non-ideal transmitting and receiving elements should be carried out. In particular, the operating bandwidth of real antenna arrays is limited, and the radiated power is strongly linked to this interval. In general terms, the radiation efficiency of the transmitting antenna system is defined as:

$$\eta_T = \frac{P_T}{P_A} \tag{18}$$

Where $P_A$ is the total available input power, and $P_T$ is the effective radiated power that depends on the transmitting antenna bandwidth. Therefore, the power loss evaluation considers the effective amount of bandwidth available in transmission, outside this frequency range no radiation occurs. The total average signal power $P_x$ has been measured over a band of 300 $MHz$, that coincides with the bandwidth of the 4-monopoles array prototype used as transmitter. This value has been set as denominator in the $P_{loss}$ equation (14), and several measurements have been performed varying $B_w$ (i.e. measuring different levels of $P_{B_w}$). Maintaining the same operating conditions described in section IV, and fixing the pulse duty-cycle to 0.1, a straight comparison of the simulated and measured $P_{loss}$ curves is reported in Fig. 13.

As can be observed from the plots, the simulated and measured curves show the same trends and confirm the theoretical predictions: indeed, as the bandwidth increases, $P_{loss}$ decreases since a higher amount of harmonic power is distributed within $B_w$. Fig 14 shows the comparison of the $P_{loss}$ (measured results only, for the sake of the figure clarity) resulting not only from the different modulating pulses shapes, but also from the pulse durations: an increase of $f_p$ (hence, a reduction of the pulse duration) negatively impacts on the loss of power.

From these measurement comparisons, some concluding remarks can be drawn. Firstly, by adopting a time control based on the rectangular pulse, a significant $P_{loss}$ reduction is obtained by reducing $f_p$ from $20\,MHz$ to $5\,MHz$. These results validate the novel idea of exploiting the harmonic radiations to enhance the effectiveness of TCFDA systems for WPT purposes. Secondly, if $f_p = \Delta f = 5\,MHz$ is chosen, the raised cosine pulse waveform with $\alpha = 1$ allows for the best $P_{loss}$ minimization. As a representative example, let us assume $B_w = 100\,MHz$, $d = 0.1$ and consider different values of $f_p$ and different pulse shapes: the corresponding simulated and measured $P_{loss}$ are derived and reported in Table I.

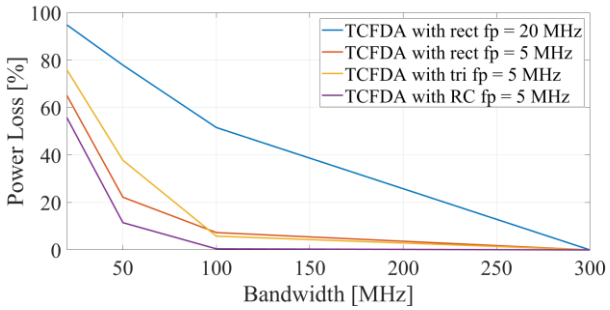


Fig. 14. Measured Power Loss vs bandwidth, for different pulse shapes.

The obtained values help a designer in the choice of TCFDA degrees of freedom: as discussed in Section III, the frequency offset $\Delta f$ defines the FDA pattern periodicity (equal to $1/\Delta f$), and it has an impact on the focusing direction whose precise value is set by the couple $(\tau, T_{on})$; on the other hand, $\Delta f$ does not affect the harmonic content discussed in this work, which strongly depends on the choice of the pulse frequency $f_p$, as clearly shown by the first two rows of Table I. As a concluding remark, the present analysis fixes $f_p = \Delta f$ as the best solution to fulfil the main TCFDA performance requirements, namely the minimization of $P_{loss}$ for advanced WPT applications.

TABLE I
POWER LOSS LEVELS ($d = 0.1$, $B_w = 100\,MHz$)

| Pulse | Simulation | Measurement |
|---|---|---|
| *Rectangular* ($f_p = 20\,MHz$) | 53.31 % | 54.58 % |
| *Rectangular* ($f_p = 5\,MHz$) | 9.09 % | 10.32 % |
| *Triangular* ($f_p = 5\,MHz$) | 5.43 % | 5.91 % |
| *Raised cosine* ($f_p = 5\,MHz$) | 0.48 % | 0.76 % |

## VII. CONCLUSION

The favorable exploitation of the harmonic generation in time-controlled FDA for WPT purposes is theoretically

investigated and experimentally demonstrated. Through this analysis, a comparison among different and new driving pulses is possible: the triangular pulse seems to be the best choice for future TCFDA systems, offering the best trade-off between radiation accuracy and $P_{loss}$. By means of the dynamic control of the design parameters of the pulse (width and delay) and by setting its periodicity coincident with that one of the FDA radiation phenomena, the selective and target-aware far-field transmission of power becomes a concrete possibility. Future works may be oriented towards a quantitative investigation on the power transfer capability of TCFDA, and how this task can be optimized through an ad-hoc selection of the design parameters, according to the application of interest.

## REFERENCES


[1] F. Cangialosi, T. Grover, P. Healey, T. Furman, A. Simon, and S. M. Anlage, "Time reversed electromagnetic wave propagation as a novel method of wireless power transfer," in *2016 IEEE Wireless Power Transfer Conference (WPTC)*, Aveiro, Portugal, 2016, pp. *1-4*.

[2] D. Belo, D. C. Ribeiro, P. Pinho, and N. Borges Carvalho, "A selective, tracking, and power adaptive far-field wireless power transfer system," *IEEE Trans. Microw. Theory Tech*., vol. *67*, no. *9*, pp. *3856-3866*, Sept. 2019.

[3] D. Masotti, A. Costanzo, M. Del Prete, and V. Rizzoli, "Time-modulation of linear arrays for real-time reconfigurable wireless power transmission," *IEEE Trans. Microw. Theory Tech.*, vol. *64*, no. *2*, pp. *331-342*, Feb. 2016.

[4] P. Antonik, M. C. Wicks, H. D. Griffiths, and C. J. Baker, "Frequency diverse array radars," in *2006 IEEE Conference on Radar*, Verona, NY, USA, 2006, pp. *3* pp.-..

[5] W. -Q. Wang, "Retrodirective frequency diverse array focusing for wireless information and power transfer," *IEEE J. Sel. Areas Commun*., vol. *37*, no. *1*, pp. *61-73*, Jan. 2019.

[6] E. Fazzini, A. Costanzo, and D. Masotti, "Ranging on-demand microwave power transfer in real-time," *IEEE Microw. Wireless Comp. Lett.*, vol. *31*, no. *6*, pp. *791-793*, Jun. 2021.

[7] Y. Liao, W. -q. Wang, and H. Shao, "Symmetrical logarithmic frequency diverse array for target imaging," *in 2018 IEEE Radar Conference (RadarConf18)*, Oklahoma City, OK, USA, 2018, pp. *0039-0042*.

[8] A. Akkoç, E. Afacan, and E. Yazgan, "Investigation of planar frequency diverse array antenna in concentric circular geometry," in *2019 11th International Conference on Electrical and Electronics Engineering (ELECO)*, Bursa, Turkey, 2019, pp. *651-654*.

[9] E. Fazzini, A. Costanzo, and D. Masotti, "A new wheel-spoke transmitter for efficient WPT based on frequency diversity," in *2022 52nd European Microwave Conference (EuMC)*, Milan, Italy, 2022, pp. *576-579*.

[10] W. Khan, I. M. Qureshi, and S. Saeed, "Frequency diverse array radar with logarithmically increasing frequency offset," *IEEE Antennas Wireless Propag. Lett.*, vol. *14*, pp. *499-502*, 2015.

[11] W. Choi, A. Georgiadis, M. M. Tentzeris, and S. Kim, "Analysis of exponential frequency-diverse array for short-range beam-focusing technology," *IEEE Trans. Antennas Propag.*, vol. *71*, no. *2*, pp. *1437-1447*, Feb. 2023.

[12] R. Çetiner, Ş. Demir, and A. Hizal, "Range and angle measurement in a linear pulsed frequency diverse array radar," in *2017 IEEE Radar Conference (RadarConf)*, Seattle, WA, USA, 2017, pp. *0064-0067*.

[13] A. -M. Yao, W. Wu, and D. -G. Fang, "Frequency diverse array antenna using time-modulated optimized frequency offset to obtain time-invariant spatial fine focusing beampattern," *IEEE Trans. Antennas Propag.*, vol. *64*, no. *10*, pp. *4434-4446*, Oct. 2016.

[14] J. Huang, K. -F. Tong, and C. Baker, "Frequency diverse array: simulation and design," in *2009 Loughborough Antennas & Propagation Conference*, Loughborough, UK, 2009, pp. *253-256*.

[15] Y. Xu, X. Shi, J. Xu, and P. Li, "Range-angle-dependent beamforming of pulsed frequency diverse array," *IEEE Trans. Antennas Propag.*, vol. *63*, no. *7*, pp. *3262-3267*, Jul. 2015.

[16] B. Chen, X. Chen, Y. Huang, and J. Guan, "Transmit beampattern synthesis for the FDA radar," *IEEE Antennas Wireless Propag. Lett.*, vol. *17*, no. *1*, pp. *98-101*, Jan. 2018.

[17] M. Tan, C. Wang, and Z. Li, "Correction analysis of frequency diverse array radar about time," *IEEE Trans. Antennas Propag.*, vol. *69*, no. *2*, pp. *834-847*, Feb. 2021.

[18] H. E. Shanks, and R. W. Bickmore, "Four dimensional electromagnetic radiators," *Can. J. Phys.*, vol. *37*, no. *3*, pp. *263–275*, 1959.

[19] W. H. Kummer, A. T. Villeneuve, T. S. Fong, and F. G. Terrio, "Ultra-low sidelobes from time-modulated arrays," *IEEE Trans. Antennas Propag.*, vol. *11*, no. *6*, pp. *633–639*, Nov. 1963.

[20] D. Masotti, A. Costanzo, M. Del Prete, and V. Rizzoli, "Time-modulation of linear arrays for real-time reconfigurable wireless power transmission," *IEEE Trans. Microw. Theory Tech.*, vol. *64*, no. *2*, pp. *331-342*, Feb. 2016.

[21] R. González Ayestarán, M. R. Pino, P. Nepa, and B. Imaz-Lueje, "Multi-user near-field focusing through time-modulated arrays," *IEEE Trans. Antennas Propag.*, vol. *70*, no. *5*, pp. *3374-3384*, May 2022.

[22] J. C. Bregains, J. Fondevila, G. Franceschetti, and F. Ares, "Signal radiation and power losses of time-modulated arrays," *IEEE Trans. Antennas Propag.*, vol. *56*, No. *6*, pp. *1799-1804*, Jun. 2008.

[23] I.Kanbaz, U. Yesilyurt, S. Kuzu, and E. Aksoy, "Total harmonic power of arbitrarily switched nonuniform period time-modulated arrays," *IEEE Antennas Wireless Propag. Lett.*, vol. *19*, no. *1*, pp. *193–197*, Jan. 2020.

[24] A. M. Jones and B. D. Rigling, "Planar frequency diverse array receiver architecture," in *2012 IEEE Radar Conference*, Atlanta, GA, USA, 2012, pp. *0145-0150*.

[25] Y. Xu, X. Shi, J. Xu and P. Li, "Range-angle-dependent beamforming of pulsed frequency diverse array," *IEEE Trans. Antennas Propag.*, vol. *63*, no. *7*, pp. *3262-3267*, Jul. 2015.

[26] D. Masotti, A. Costanzo, P. Francia, M. Filippi, and A. Romani, "A load-modulated rectifier for RF micropower harvesting with start-up strategies," *IEEE Trans. Microw. Theory Tech.*, vol. *62*, no. *4*, pp. *994-1004*, Apr. 2014.

[27] M. Del Prete, A. Costanzo, M. Magno, D. Masotti and L. Benini, "Optimum excitations for a dual-band microwatt wake-up radio," *IEEE Trans. Microw. Theory Tech.*, vol. *64*, no. *12*, pp. *4731-4739*, Dec. 2016.


**Tommaso Tiberi** (Student Member, IEEE) received the M.Sc. degree in Telecommunications Engineering from the University of Bologna, Bologna, Italy, in 2022. He is currently pursuing the Ph.D. degree in electronics, telecommunications, and information technologies engineering. In January 2023, he joined the Department of Electrical, Electronic and Information Engineering "G. Marconi," University of Bologna as a Research Fellow within the framework of the PRIN WPT4WID ("Wireless Power Transfer for Wearable and Implantable Devices") Project. His research interests include the design of advanced radiating architectures exploiting frequency diversity and waveforms engineering for precise and dynamic wireless power transfer systems.

**Enrico Fazzini** (Student Member, IEEE) received the M.Sc. degree in Telecommunications Engineering from the University of Bologna, Bologna, Italy, in 2020. He is currently pursuing the Ph.D. degree in electronics, telecommunications, and information technologies engineering. In 2020, he joined the Department of Electrical, Electronic and Information Engineering "G. Marconi," University of Bologna as a Research Fellow within the framework of the PRIN WPT4WID ("Wireless Power Transfer for Wearable and

Implantable Devices") Project. His research interests include the design of wireless power transfer systems operating at microwaves and millimeter waves with focusing on smart power transmitter, especially Time Modulated and Frequency Diverse Arrays.

**Alessandra Costanzo** (Fellow, IEEE) has been a Full Professor at the Alma Mater Studiorum, Università di Bologna, Bologna, Italy, since 2018, where she leads the RF and Wireless Laboratory.

She is also involved in research activities dedicated to design entire wireless power transmission systems based on the combination of electromagnetic (EM) and nonlinear numerical techniques, adopting both far- and near-field solutions, for several power levels and operating frequencies. She was the Co-Founder of the EU COST action IC1301 WiPE "Wireless power transfer for sustainable electronics." She has authored more than 260 scientific publications on peer-reviewed international journals and conferences and several chapter books. She owns four international patents. Prof. Costanzo is the past Chair of the MTT-26 Committee on Wireless Energy Transfer and Conversion from 2016 to 2017 and a member of the MTT-24 Committee on radiofrequency identification (RFID). She is a past Associate Editor of the IEEE TRANSACTIONS ON MICROWAVE THEORY AND TECHNIQUES and the *International Journal of Microwave and Wireless Technologies* (Cambridge). Since 2016, she has been the Steering Committee Chair of the IEEE JOURNAL OF RADIO FREQUENCY IDENTIFICATION. She is an MTT-S representative and Distinguished Lecturer of the CRFID, where she has been appointed as the Chair of EUMC2022.

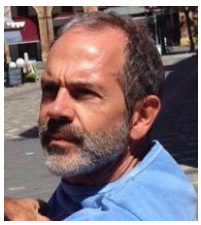

**Diego Masotti** (Senior Member, IEEE) received the Ph.D. degree in electric engineering from the University of Bologna, Bologna, Italy, in 1997. In 1998 he joined the University of Bologna, where he is currently an Associate Professor of electromagnetic fields. His research interests are in the areas of nonlinear microwave circuit simulation and design, with emphasis on nonlinear/electromagnetic codesign of integrated radiating subsystems/systems for wireless power transfer and energy harvesting applications. He authored more than 80 scientific publications in peer-reviewed international journals and more than 180 scientific publications on proceedings of international conferences.

Dr. Masotti is a member of the Paper Review Board of the main Journals of the microwave sector. He serves on the Editorial Board of the *International Journal of Antennas and Propagation*, the *Journal of Wireless Power Transfer*, IEEE ACCESS, and *Electronics Letters*.